

Quenching a UCST Polymer Blend into Phase Separation by Local Heating

A. Voit, A. Krekhov, and W. Köhler*

Physikalisches Institut, Universität Bayreuth,
D-95440 Bayreuth, Germany

Received September 22, 2006

Phase separation of polymer blends, especially spinodal decomposition, has fascinated researchers for a long time, and a large body of both experimental and theoretical papers can be found in the literature. Almost all authors describe the phase behavior of the blend by means of an equilibrium phase diagram, where the locus of the mixture is fully characterized by its average composition and a constant temperature.

Comparatively little work has been done on the phase behavior of polymer blends subject to nonuniform temperature fields. Lee et al. studied spinodal decomposition in the presence of a temperature gradient,^{1,2} and Tanaka et al. studied the influence of periodically driving the polymer mixture above and below the instability point.³

An interesting approach based on combinatorial methods has recently been presented by Meredith et al.⁴ Both for scientific investigations and technological applications the precise knowledge of the phase behavior of polymer blends is a prerequisite. Establishing the phase diagram is, however, a tedious task, requiring significant amounts of material and several individual experiments for the determination of the cloud point curve. According to these authors, the task can significantly be simplified by employing a continuous combinatorial library which should allow for the determination of the entire cloud point curve in a single-shot experiment. The library consists of a thin film of the blend with a constant composition gradient on a flat substrate. Perpendicular to this composition gradient a constant temperature gradient is applied across the film, pointing along the lines of constant composition. After a few hours of annealing, the phase diagram can be directly read from the polymer film.

In the following we will demonstrate that the basic assumption of all experiments and simulations in refs 1–4, the assumption that equilibrium phase diagrams can be applied to nonequilibrium situations, is generally not true. In the presence of an inhomogeneous temperature field, the position of a small volume element of the sample within the equilibrium phase diagram is no longer determined by its local temperature and the average composition of the blend. Temperature gradients lead to a change of the local composition of multicomponent systems due to the Soret effect (thermal diffusion).⁵ As a consequence, composition and temperature cannot be viewed as orthogonal coordinates. The position within the phase diagram on the composition axis becomes a function both of the spatial wavelengths contained in the temperature field and of the time elapsed.

In the one-phase region the coupling between temperature and concentration c (weight fractions) is accounted for by an extension of Fick's second law of diffusion:⁶

$$\partial_t c = \nabla[D\nabla c + c(1-c)D_T\nabla T] \quad (1)$$

D and D_T are the collective and the thermal diffusion coefficient, respectively. Their ratio $S_T = D_T/D$ is a measure for the amplitude of the concentration change induced by the temperature gradient in the stationary state. Close to the critical point, diffusion slows down by orders of magnitude. S_T diverges, and the coupling between temperature gradient and composition becomes very strong.^{7,8} S_T values up to 20 K⁻¹ have been reported for poly(dimethylsiloxane)/poly(ethylmethylsiloxane) (PDMS/PEMS) blends.^{9,10} The coexistence line in a ternary system, a solution of a polymer blend, can be shifted by 20 K in the presence of a temperature gradient.¹¹ Lalaud et al.¹² and Delville et al.^{13,14} have demonstrated that micellar microemulsions can be driven into phase separation in confined geometries by utilizing electrostriction and the Soret effect. Platten et al.¹⁵ and Assenheimer et al.¹⁶ studied the interplay between phase separation and convection of a binary mixture exposed to a temperature gradient.

The dramatic influence of an inhomogeneous temperature field on the phase behavior of a PDMS($M_w = 16.4$ kg/mol)/PEMS($M_w = 48$ kg/mol) blend, the only comparable system where the thermal diffusion and Soret coefficients are known so far (Figure 1), is demonstrated in the following. The samples are 100 μm thick layers of the polymer mixture with off-critical PDMS equilibrium weight fractions of $c_0 = 0.3$ and $c_0 = 0.9$. The polymer is slightly colored with quinizarin, and a galvano mirror driven by a sawtooth voltage is used to scan a focused laser ($\lambda = 515$ nm) across the sample. The absorbed energy thermalizes and heats the sample along the line written by the laser. Initially, the compositions and the temperatures are such that the two samples are in the one-phase region. The two filled circles mark the initial positions to the left and to the right of the binodal (Figure 2).

Since the phase diagram shows a lower miscibility gap with a critical composition of $c_{\text{crit}} = 0.61$, heating alone would never be able to quench the polymer blend into phase separation. Because of the Soret effect, however, local heating is unavoidably accompanied by concentration changes, and a volume element within the center of the line written by the laser experiences an enrichment of the thermophilic PDMS. Consequently, this volume element will be displaced not only vertically in the phase diagram toward a higher temperature but also horizontally toward higher c . Provided the coupling is strong enough, the volume element to the left of the binodal (at $c = 0.3$) will eventually cross the phase boundary, and phase separation by nucleation and growth will set in. This is shown in the upper part of Figure 3. The phase contrast micrograph is such that a lower refractive index appears brighter and vice versa. Since PDMS ($n = 1.402$ at $T = 293$ K) has a lower refractive index than PEMS ($n = 1.429$ at $T = 293$ K), the diffuse line with an increased PDMS concentration and the phase-separated PDMS-rich droplets appear brighter. Since these droplets are of lower refractive index than the surrounding medium, optical tweezing cannot occur. Around the bright line there is a faint dark halo indicating PEMS enrichment in this region. In order to get insight into concentration and temperature distribution, 3-d simulations of eqs 1 and 2 for the polymer layer of thickness 100 μm and lateral dimensions 1 mm \times 1 mm confined between 1 mm thick sapphire plates have been performed using finite differences with adaptive mesh refinement technique. It has been found that PEMS accumulation does not occur in the center of the cuvette, but rather on the sapphire

* Corresponding author. E-mail: werner.koehler@uni-bayreuth.de.

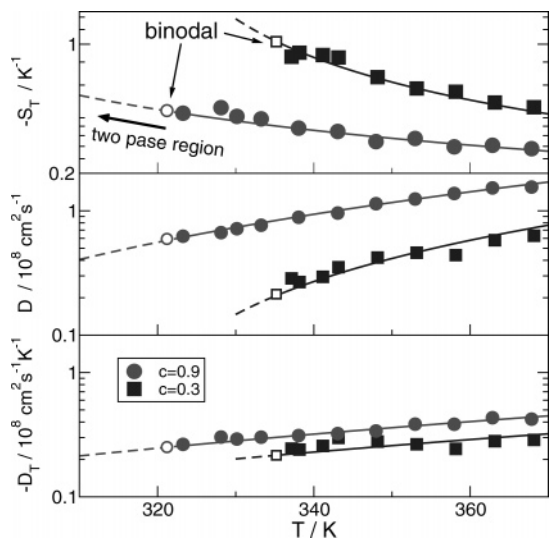


Figure 1. S_T , D , and D_T of a PDMS/PEMS (16.4/48 kg/mol) blend for two PDMS weight fractions ($c = 0.3$, $c = 0.9$) investigated as functions of temperature in the one-phase region. The dashed lines are extrapolated into the two-phase region. The open symbols mark the binodal. The measurements have been performed by a transient holographic grating technique described elsewhere.¹⁹

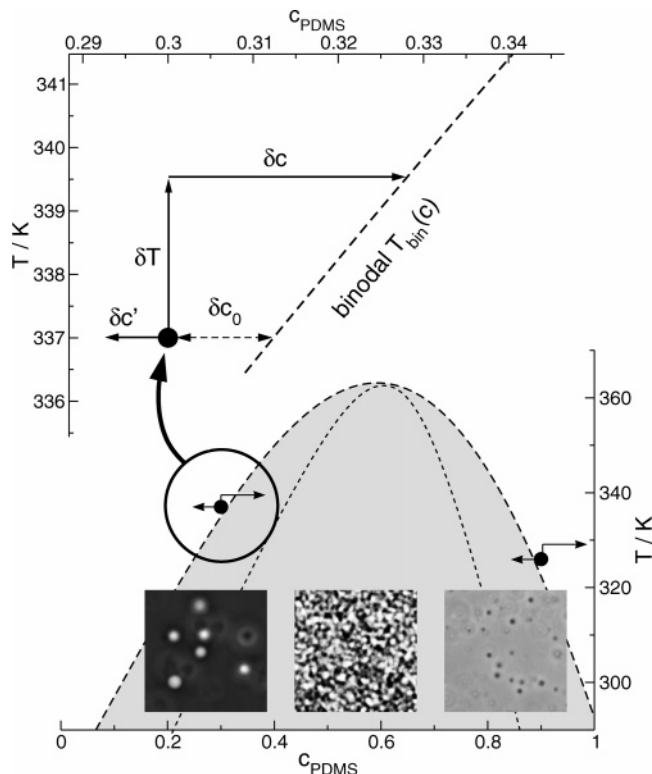


Figure 2. Phase diagram of the PDMS/PEMS blend. The binodal has been obtained by a fit to turbidity measurements. The spinodal is only a guess. The initial positions of the two samples are marked by filled circles. The field of view of the micrographs is $70 \times 70 \mu\text{m}^2$. They show characteristic binodal and spinodal demixing patterns after homogeneous quenches.

cell windows where the temperature is kept constant, representing the “cold side”. The displacement of a volume element within the PEMS accumulation region is indicated with $\delta c'$ in Figure 2.

Since heat diffuses much faster than mass, the temperature distribution reaches its stationary state very rapidly, and the distance to the binodal first increases. This corresponds to a shift in the vertical direction along a line of constant c . Then,

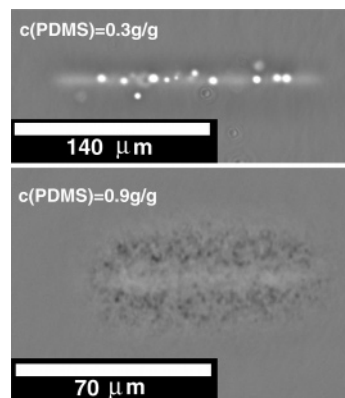


Figure 3. Phase contrast microscopy images of lines written by a scanning laser into the PDMS/PEMS blend with initial concentrations to the left (upper) and to the right (lower) of the binodal (see Figure 2).

thermal diffusion sets in and locally drives the sample toward higher c along a line of constant T . The question as to whether the binodal line $T_{\text{bin}}(c)$ can be reached at all, and if so, what is the time required for that, depends on the initial distance to the binodal δc_0 along the concentration axis, the thermal diffusion coefficient D_T , and the slope of the binodal, dT_{bin}/dc . The minimum time required can be estimated as follows.

The stationary solution of the heat equation

$$\partial_t T = D_{\text{th}} \Delta T + \frac{\alpha}{\rho c_p} I \quad (2)$$

gives

$$\Delta T = -\frac{\alpha}{\kappa} I \quad (3)$$

$I(\vec{r})$ is the laser intensity, α the optical absorption coefficient, ρ the density, c_p the specific heat, κ the thermal conductivity, and $D_{\text{th}} = \kappa(\rho c_p)^{-1}$ the thermal diffusivity.

Inserting eq 3 into eq 1 yields for short times, where the concentration change is small ($\Delta c \approx 0$) and $D \approx \text{constant}$

$$\partial_t c = -\frac{\alpha}{\kappa} D_T c_0 (1 - c_0) I \quad (4)$$

If the sample temperature within the center of the line rises by δT , the distance to the binodal before thermal diffusion sets in is

$$\delta c = \delta c_0 + \delta T \left(\frac{dT_{\text{bin}}}{dc} \right)^{-1} \quad (5)$$

$\delta T = 2.5$ K has been determined from a full 3d simulation of the thermal problem, since boundary conditions have to be taken properly into account for the stationary temperature distribution. As saturation effects will always slow down the evolution of the concentration profile, the minimum time δt to reach the binodal can be estimated from the linear growth in the short time limit:

$$\delta t = \delta c / \partial_t c = -\frac{\delta c_0 + \delta T (dT_{\text{bin}}/dc)^{-1}}{D_T c_0 (1 - c_0) \alpha / \kappa} \quad (6)$$

The laser power was 5 mW, which was distributed over a $2 \times 200 \mu\text{m}^2$ area in the focus of the laser, thereby averaging over the fast modulation from the repetitive (20 Hz) scanning of the line. This corresponds to an average intensity of $I = 1.25 \times$

10^7 W m^{-2} . The other parameters are $c_0 = 0.3$, $\delta c_0 = 0.012$, $\alpha = 500 \text{ m}^{-1}$, $\kappa = 0.16 \text{ W (K m)}^{-1}$, $D_T = -2.5 \times 10^{-13} \text{ m}^2 (\text{s K})^{-1}$, and $dT_{\text{bin}}/dc = 166 \text{ K}$. Since PDMS is thermophilic, its thermal diffusion coefficient is negative. Inserting the above numbers into eq 6 yields a lower limit for the minimum time until the two-phase region can be reached of $\delta t \approx 13 \text{ s}$. If the starting point is chosen directly on the binodal ($\delta c_0 = 0$), δt reduces to 7.3 s and becomes independent of the laser power within linear approximation. Once the binodal has been crossed, additional time is needed for nucleation and growth of the droplets until they are sufficiently large to become visible in the microscope.^{17,18} In the experiment, first droplets appeared after 7 min, which is significantly longer than the minimum time estimated.

As expected, no phase separation could be induced in the center of the heated line for $c = 0.9$, since thermal diffusion here drives the heated regions deeper into the homogeneous phase. Again, PEMS enrichment occurs close to the windows in the region around the heated line and leads to an excursion toward lower c without noticeable temperature rise. As can be seen from the lower part of Figure 3, this is sufficient to cross the phase boundary now within the halo.

Note that PDMS-rich phases show up as bright and PEMS-rich phases as dark regions in the phase contrast micrographs. This is also illustrated by the insets in Figure 2 which have been obtained by thermally quenching the entire sample homogeneously into the binodal region on the low (left) and high (right) concentration side. On the low concentration side, the nucleating droplets correspond to the PDMS rich phase and vice versa. Within the binodal the spinodal region can be found. Here, the demixing pattern originating from spinodal decomposition is completely different from the one obtained by nucleation and growth within the metastable regions between binodal and spinodal. The middle micrograph inserted in Figure 2 has been obtained after a quench below the spinodal. From a comparison of these demixing patterns with the ones obtained by local laser heating it is immediately clear that in the latter the sample has been driven across the binodal but not across the spinodal. Since in all cases the position of the sample within the phase diagram, based on its average composition and temperature, is above the binodal within the one-phase region, all induced structures disappear slowly by diffusion after the laser is switched off.

As we have demonstrated, a polymer blend in an inhomogeneous field cannot be treated in terms of a quasi-equilibrium system where only the local temperature varies, since temperature and concentration are unavoidably coupled in a complex and time-dependent manner. Since the purpose of the combinatorial library discussed in the introduction is the establishment

of the phase diagram, the behavior in the vicinity of the phase boundary, especially near the critical point, is of utmost importance. It is exactly there, however, where the Soret coefficient diverges, and already small temperature differences can lead to large concentration shifts. Additional complications will arise from a competition between diffusion and phase-separation time scales. It may be possible to identify parameters where these time scales are sufficiently separated and thermal diffusion is slow enough to be negligible compared to phase separation. This would provide a window where such a technique can safely be applied. The comparison with cloud point data measured by laser light scattering in ref 4 indicates that the measurements have been carried out within this experimental window, although thermal diffusion had not been taken into consideration for the design and analysis of the experiment. For a serious estimation, the thermal diffusion and Soret coefficients of the blend are required within the entire phase diagram. To our knowledge, however, PDMS/PEMS is the only polymer blend where these numbers are known so far.

Acknowledgment. We thank G. Meier for providing the samples. This work was supported by the Deutsche Forschungsgemeinschaft (SFB481/A8).

References and Notes

- (1) Lee, K.-W. D.; Chan, P. K.; Feng, X. *Macromol. Theory Simul.* **2002**, *11*, 996.
- (2) Lee, K.-W. D.; Chan, P. K.; Feng, X. *Macromol. Theory Simul.* **2003**, *12*, 413.
- (3) Tanaka, H.; Sigehezi, T. *Phys. Rev. Lett.* **1995**, *75*, 874.
- (4) Meredith, J. C.; Karim, A.; Amis, E. J. *Macromolecules* **2000**, *33*, 5760.
- (5) Soret, C. *Arch. Geneve* **1879**, *3*, 48.
- (6) de Groot, S. R.; Mazur, P. *Non-equilibrium Thermodynamics*; Dover: New York, 1984.
- (7) Giglio, M.; Vendramini, A. *Phys. Rev. Lett.* **1975**, *34*, 561.
- (8) Pohl, D. W. *Phys. Lett. A* **1980**, *77*, 53.
- (9) Enge, W.; Köhler, W. *Phys. Chem. Chem. Phys.* **2004**, *6*, 2373.
- (10) Voit, A.; et al. *Phys. Rev. Lett.* **2005**, *94*, 214501.
- (11) Kumaki, J.; Hashimoto, T.; Granick, S. *Phys. Rev. Lett.* **1996**, *77*, 1990.
- (12) Lalaude, C.; Delville, J. P.; Buil, S.; Ducasse, A. *Phys. Rev. Lett.* **1997**, *78*, 2156.
- (13) Delville, J. P.; Freysz, E.; Sarger, L.; Ducasse, A. *J. Phys. II* **1993**, *3*, 297.
- (14) Delville, J. P.; Lalaude, C.; Buil, S.; Ducasse, A. *Phys. Rev. E* **1999**, *59*, 5804.
- (15) Platten, J. K.; Chavepeyer, G. *Physica A* **1995**, *213*, 110.
- (16) Assenheimer, M.; Khaykovich, B.; Steinberg, V. *Physica A* **1994**, *208*, 373.
- (17) Tokuyama, M.; Enomoto, Y. *Phys. Rev. Lett.* **1992**, *69*, 312.
- (18) Cumming, A.; Wiltzius, P.; Bates, F. S. *Phys. Rev. Lett.* **1990**, *65*, 863.
- (19) Wittko, G.; Köhler, W. *Philos. Mag.* **2003**, *83*, 1973.

MA062205J